The Bidirectional Reflectance of Black Silicon Used in Space and Earth Remote Sensing Applications

Georgi T. Georgiev, James J. Butler, Ron Shiri, Christine A. Jhabvala, Edward J. Wollack, Elena M. Georgieva

NASA Goddard Space Flight Center, Greenbelt, MD 20771, e-mail: georgi.t.georgiev@nasa.gov

ABSTRACT

Space-based astrophysical and remote sensing observations often require the detection and measurement of light originating from distant and relatively faint objects. These observations are highly susceptible to scattered light which may introduce imaging artifacts, obscure object details, and increase measurement noise. This paper describes the initial work of characterizing representative black materials used in coronagraph instruments and other spaceborne instruments. Measurements of "blackness" and the achieved reflectance of black silicon are provided in the spectral range from 400nm to 2500nm using 8° directional hemispherical measurements. The bidirectional reflectance of black silicon was also measured at discrete wavelengths, 633nm, and 1064nm, using the optical scatterometer located at NASA Goddard Space Flight Center's Diffuser Calibration Laboratory (DCL). A 100mm diameter black silicon sample was fabricated and optically characterized. The BRDF of other well-known black materials such as Z306 and Fractal Black are also presented and discussed.

Keywords: Bidirectional Reflectance Distribution Function (BRDF), Calibration, Black Silicon, Reflectance, Remote Sensing.

1. INTRODUCTION

Satellite-based earth and space observations present scientists and engineers with two extreme challenges in remote sensing. From low orbit, the Earth appears as a bright target of large angular extent. Quantitative remote sensing of that part of the Earth within the field of view of a satellite instrument is comprised of light both within and outside the instrument field of view. This is often termed the size of source effect. Light which enters the instrument is then diffracted and scattered by internal instrument structures, adversely impacting remote sensing measurements. In contrast, space-based astrophysical observations often require the detection and measurement of light originating from small, distant, often faint objects. Imaging and spectral characterization of faint exoplanets orbiting around bright stars requires advanced coronagraph techniques to suppress the host starlight in the image plane of a telescope. The direct imaging of exoplanets often require fabricated coronagraph masks to control scattering and diffraction of light. The NASA Wide Field Infrared Telescope (WFIRST) mission includes a coronagraph instrument to enable such objectives[1]. These observations are also highly sensitive to scattered light which can obscure the remotely sensed object and elevate the measurement noise. Scattered light is often controlled by the use of light tight enclosures equipped with strategically placed baffles and stops. In addition to placement, achieving a low bidirectional reflectance from these baffling structures is key in the

reduction of scattered light within an instrument. The ideal surface for controlling of stray light would be a Lambertian absorber achieving a uniform low reflectance independent of light incident angle and the wavelength. Internal instrument scattered light is typically reduced using a number of black surface treatments. These treatments include paints, appliques, and etched, electro-deposited and sprayed metal surfaces. Different techniques were reported so far in a number of publications, reviews, and databases on the optical properties of black surfaces and materials[2,3,4,5,6]. The choice of treatment depends strongly on the geometry and required level of glint reduction, substrate material, operating wavelength range, and, for the specialized case of space instrumentation, optical and mechanical stability in the on-orbit environment as well having low molecular outgassing.

A new and very promising black material for reducing stray light in space instruments is Black Si[7] In this work, we employed the cryogenic etching process to fabricate black silicon to achieve a high aspect ratio structure with higher etch rate than conventional reactive ion etching. We imprinted the patterned mask on a diffraction-limited silicon wafer with silver/aluminum metal applied to the reflective area. Then we used a cryogenic etching process to fabricate Black Si on the non-reflective region. Subsequent optical measurements based on the Bidirectional Reflectance Distribution Function (BRDF) of uniformly coated Black Si on silicon wafer show highly diffusive Black Si with a specular reflective component on the order of seven magnitudes lower than the total hemispherical reflectance when a polarized or non-polarized incident beam is used.

2. EXPERIMENTAL

2.1. Sample preparation

The Black Si sample is shown in Fig.1. A polished silicon surface has a typical 8° directional /hemispherical reflectance of about 35% in the visible spectrum. However the surface microstructures can significantly reduce the reflectivity through shading of the reflected light and

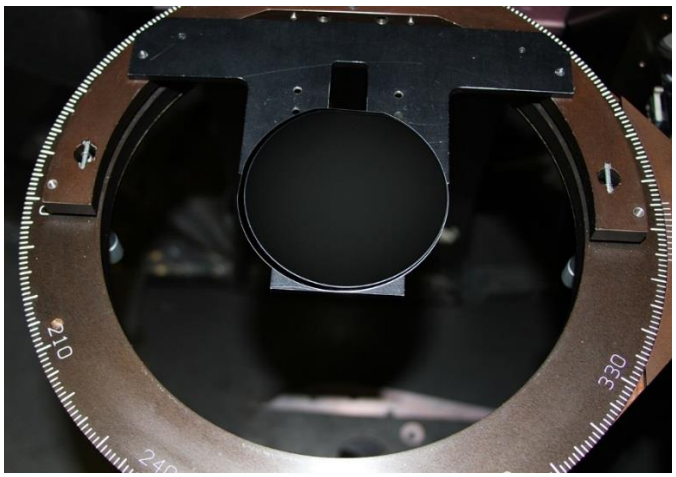

Fig.1. Black Silicon sample on the Scatterometer sample stage

obscuration of the incident light, Fig.2. The Black Si reflectance can be lowered by using different techniques to introduce microstructures to lower the reflectance of the material surface and achieve extremely low broadband reflectance. Seven parameters are used to determine the cryogenic etching of BSi: 1) the Sulfur hexafluoride (SF_6) flow rate that primarily affects ion fluoride density, 2) O_2 flow rate that increases passivation that leads to micro-masking and enabling black silicon

formation, 3) Inductively Coupled Plasma (ICP) power to increase ion density, 4) forward power that affects etch depth and removes the passivation layer, 5) chamber pressure to increase ion density, 6) chamber temperature to enable formation of passivation layer, and 7) etch duration that affects etch depth. Out of these, two parameters contribute to the formation of Black Si, the oxygen flow rate and the chamber temperature in the form of micro-masking and passivation. All of these parameters contribute to the blackness of the substrate: and one could optimize them to obtain various levels of blackness (grayscale). For instance, the etch duration of 10 minutes[8] produces sub-optimal results while increasing the duration to 20 or 30 minutes exhibits a monotonic relation between the reflectivity and etch time but as the time increases the reflectivity decreases. On the variation of ICP power (ion density), the lowest ICP power exhibits lower reflectivity up to a point. On the other hand, the reflectivity increases with temperature. As one varies these parameters, the blackness of the substrate changes producing grayscale Black Si. Additionally, as earlier studies show mid-IR and broadband far-infrared absorbers (15-300 micron) have been modeled by employing nonlinear first-degree models (Ricatti equation) given knowledge of the optical parameters and achieved absorber geometry.

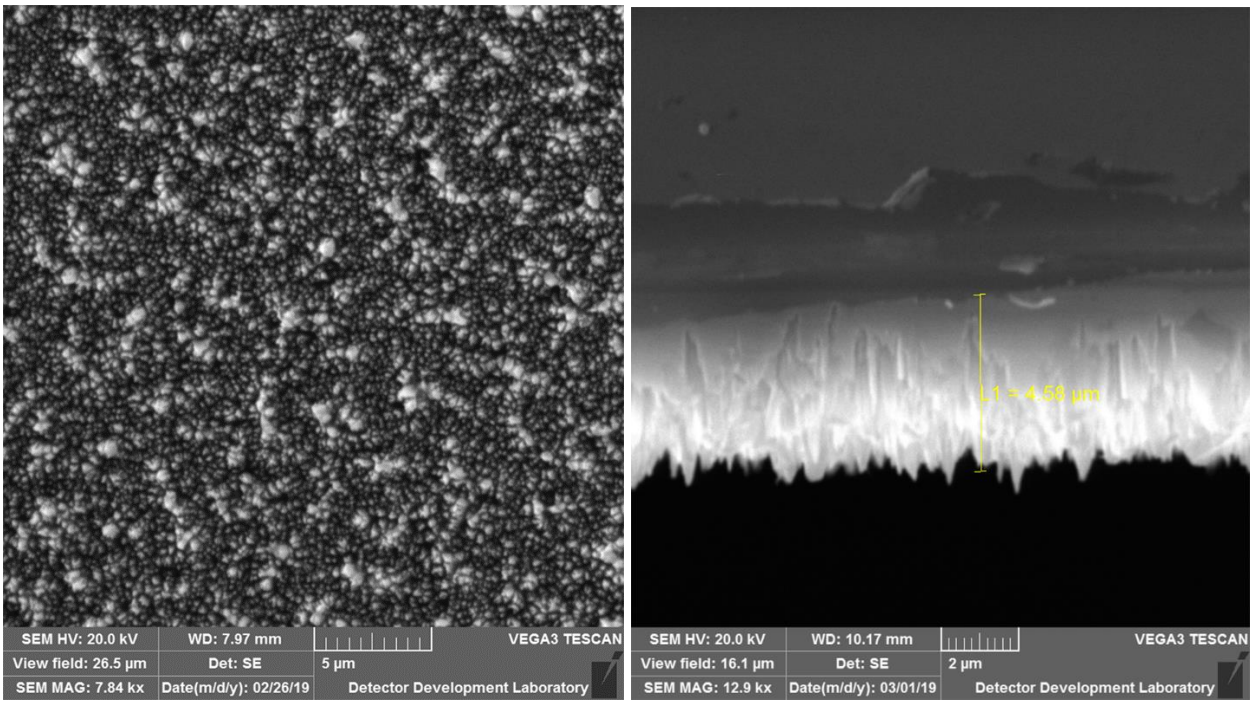

Fig.2. Scanning Electron Microscope (SEM) of cryogenic etching of black silicon on a flat Si wafer performed at the Detector Development Laboratory of Goddard Space Flight Center. (Left) Top view of the BSi and (Right) Side view of the BSi showing a 5-micron thickness height of the silicon grass or needle structures.

2.2. Optical measurements

The darkness of the Black Si sample was evaluated through measurements of their 8° directional/hemispherical reflectance from 250nm to 2500nm and their BRDF at 632.8nm and 1064nm. A Perkin Elmer 1050 spectrophotometer equipped with a 150mm Spectralon coated integrating sphere with a 25mm in diameter sample port was employed to measure the 8°directional/hemispherical reflectance of Black Si, Fractal black and Z306, Fig.3. 8° directional

/hemispherical reflectance is a measurement of all light that is scattered off of a test sample. The signal detection is performed by two detectors located inside the sphere: a R955 photomultiplier tube (PMT) for the wavelength range from 198 to 866 nm and a lead sulfide (PbS) detector to cover the 866-2500 nm spectral range. The directional/hemispherical reflectance does not discriminate the angle of reflectance but measures the total amount of reflected light. It is a very accurate measurement of the relative ability of a sample to absorb light. In this study, it is used as a screening tool to determine if a particular sample is effective at absorbing light and warrants further BRDF characterization.

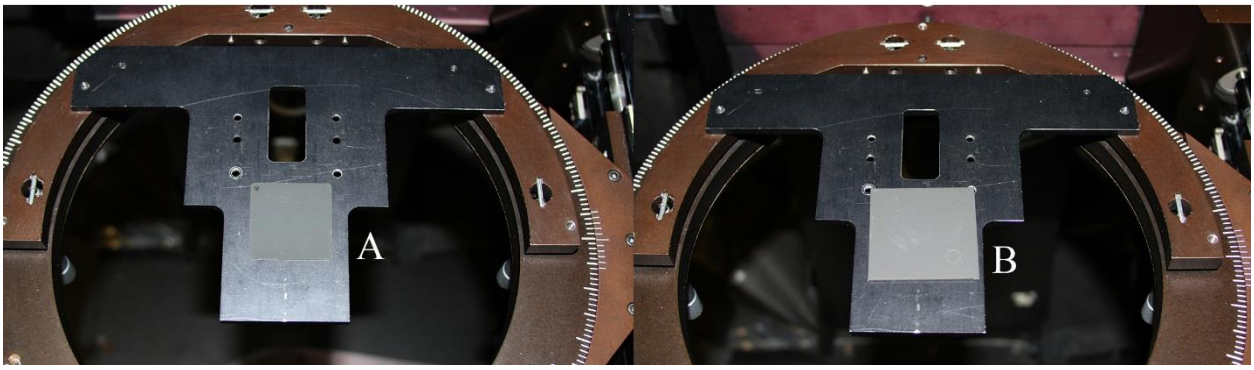

Fig.3 Reference samples on the Scatterometer sample stage, (A) Fractal black and (B) Z306

While 8° directional/hemispherical reflectance quantifies the total amount of light that is reflected over all angles, it does not provide sufficient directional information required to model stray light reaching the focal plane of an optical system. The bidirectional reflectance distribution function (BRDF) fully defines the directional reflection characteristics of a surface. It provides the reflectance of a target in a specific direction as a function of illumination and viewing geometry. The BRDF is a function of wavelength and reflects the structural and optical properties of the surface. The BRDF definition and its derivation are credited to Nicodemus et al.[9] who examined the problem of defining and measuring the scatter of diffuse and specular optical materials. Following his concept the scatter defining geometry is shown in Fig.4, where the subscripts i and s refer to incident and scatter quantities, respectively.

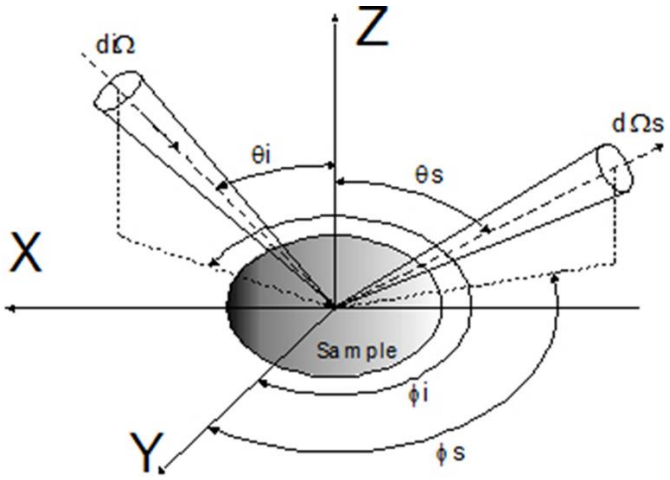

Fig.4. BRDF angular convention

Nicodemus also assumed that all scatter comes from the sample surface and none from the bulk optical media. He defined the BRDF in radiometric terms as the ratio of the surface radiance, L_s, scattered by a surface into the direction (θ_s, φ_s) to the incident surface irradiance, E_i, incident on a unit area of the surface at a particular wavelength, λ, as shown in Eq.1

$$BRDF = \frac{L_s(\theta_i, \phi_i, \theta_s, \phi_s, \lambda)}{E_i(\theta_i, \phi_i, \lambda)}, \quad (1)$$

where θ is the zenith angle, ϕ is the azimuth angle, and the subscripts *i* and *s* are for the incident and scattered (or detector) directions respectively, and λ is the wavelength. In practice, we usually present BRDF in terms of the incident power, scattered power and the geometry of the reflected scatter. It is equal to the scattered power per unit solid angle normalized by the incident power and the cosine of the detector view angle[3]:

$$BRDF = \frac{P_s / \Omega}{P_i \cos\theta_s}, \quad (2)$$

where P_s is the scatter power, Ω is the solid angle determined by the detector aperture, *A*, and the radius from the sample to the detector, *R*, or $\Omega = A/R^2$, P_i is the incident power, and θ_s is the detector zenith angle.

The definitions for describing polarized surface scattering are the same as those used in unpolarized scattering but the BRDF is expressed by matrices and the radiance and irradiance are vectors. The polarized BRDF is based on Mueller calculus and can model the polarization state of almost any surface.

The various black optical samples were measured in the Diffuser Calibration Laboratory (DCL) at NASA's Goddard Space Flight Center (GSFC) using the facility's scatterometer. The DCL is a secondary calibration facility to the primary laboratory at the National Institute of Standards and Technology (NIST). The DCL setup employs an extended silicon and InGaAs detectors a tunable coherent and supercontinuum light sources. It has provided numerous NASA projects with Bidirectional Reflectance Distribution Function (BRDF) data in the UV, Visible and the SWIR spectral regions. The scatterometer, located in a class 10000 laminar flow cleanroom, is capable of measuring the bidirectional scatter distribution function (BSDF) of a wide range of sample types including white diffusers, gray-scale diffusers, black painted or anodized diffusers, polished or roughened metal surfaces, clean or contaminated mirrors, transmissive diffusers, liquids, and granular solids. BSDF includes BRDF and the bidirectional transmissive distribution function (BTDF). The instrument is an out-of-plane optical scatterometer capable of measuring optical scatter above or below any sample. The operational spectral range of the instrument is continuous from 230 nm to 900 nm and at select laser or filter-based wavelengths in the shortwave infrared up to 2.5 microns. The scatterometer data acquisition and display is completely computer controlled.

Fig.5a presents the configuration of optical table with the following components: light source, monochromator, filter wheel, flat mirror, first spherical mirror, hard aperture, polarizer, second spherical mirror, and output mirror. For sample alignment and measurements using lasers, a laser (i.e. HeNe in the figure), quarterwave plate, chopper, laser turning mirror are used. In addition, for the laser based measurements, the polarizer is moved to a position between the laser and output turning mirrors. Figs.5b and 5c present the goniometric stages of the scatterometer. The last two

mirrors relay the monochromatic (or laser) beam through a hole in the optical table to the goniometric side of the scatterometer. The scattered light from the sample is collected by three receivers, ultraviolet-enhanced silicon from 250nm to 900nm, Indium Gallium Arsenide from 900nm to 1700nm and Extended Indium Gallium Arsenide from 1700nm to 2500nm with output fed to a computer-controlled lock-in amplifier. The sample is mounted on a stage in the horizontal plane. The sample stage allows precise positioning of the sample with respect to the incident beam and can be moved in X, Y, and Z linear directions using three motors. The sample stage provides sample rotation in the horizontal plane around the Z axis enabling changes in the incident azimuth angle, φ_i. Sample stage leveling is adjusted using two manual micrometers. Sample holders are custom designed to support samples of different sizes, shapes, and thicknesses.

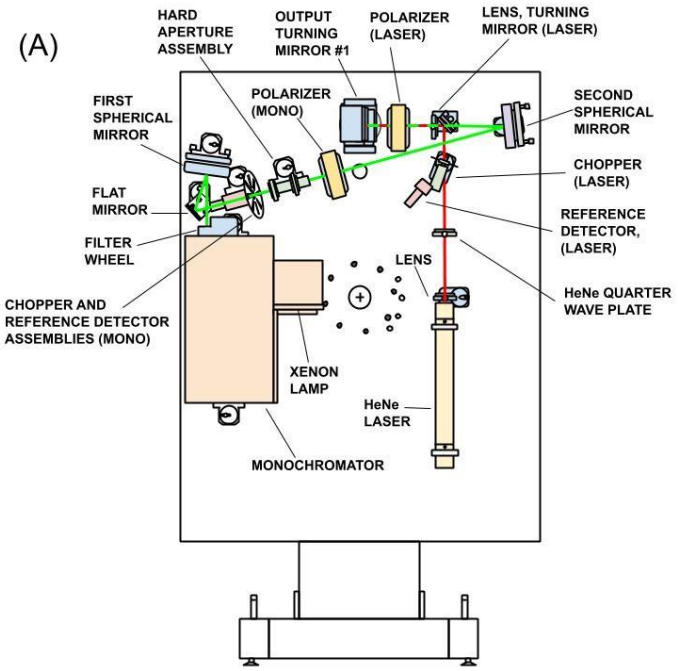

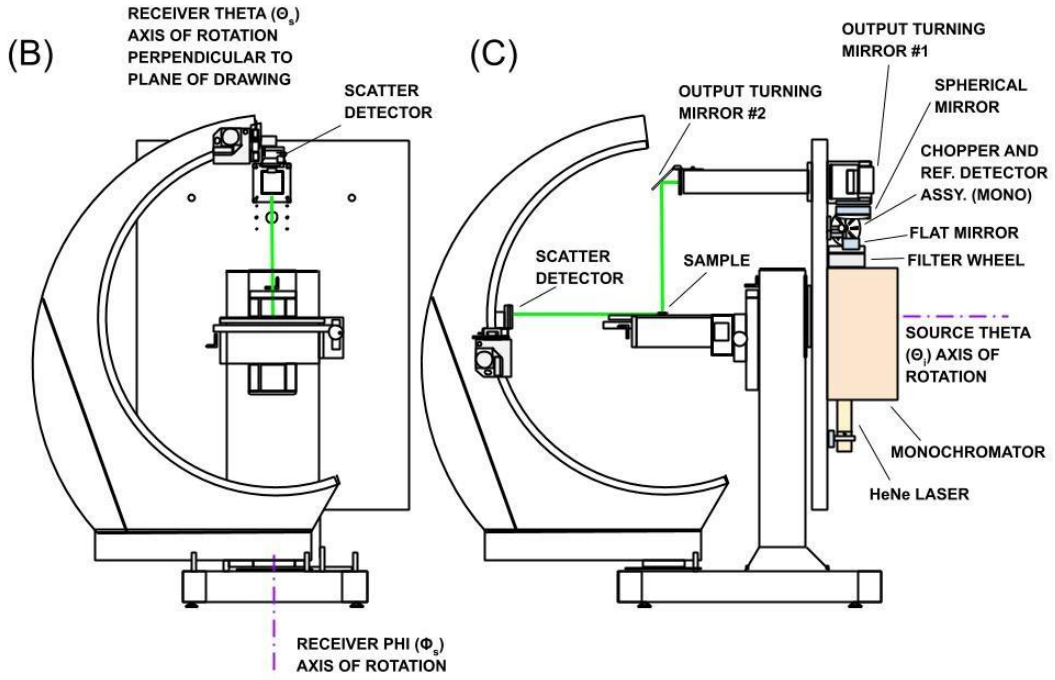

Fig. 5. The NASA scatterometer in the BRDF measuring configuration. The light source side of the scatterometer is shown in (A) and the sample side in (B). (C) is a side view showing the sample and light source sides of the instrument with the receiver φ stage rotated to a position 90° from that shown in (B).

3. RESULTS AND DISCUSSION

8° directional/hemispherical and BRDF properties of Black Si are presented in this paper. Comparisons are also made to the reflectance properties of Z306, a black paint commonly used on spaceflight surfaces and Fractal black, both used for stray light reduction.

The 8° directional/hemispherical reflectance of these samples, is plotted in Fig.6. The Black Si exhibit the lowest reflection from 250nm up to about 1000nm and then it increases to higher reflectance values. The 8° directional/hemispherical reflectance of commonly used black materials as Fractal black, and Z306 diffuse paint was measured as references. The 8° directional/hemispherical reflectance data demonstrate the extreme blackness of the Black Si sample from 250nm up to about 1000nm quantified by the total amount of light that is isotropically reflected. It is worth noting that Black Si possess the lowest hemispherical reflectance among studied black materials from 250nm to 1000nm. However, the 8° directional/hemispherical reflectance does not provide sufficient directional information required to model stray light reaching the focal plane of an optical system, which is provided by BRDF.

The BRDF fully defines the directional reflection characteristics of a surface. It provides the reflectance of a target in a specific direction as a function of illumination and viewing geometry. The BRDF is a function of wavelength and reflects the structural and optical properties of the surface. The BRDF can also be used to quantify the specularity and/or diffuseness of the Black Si and the other samples. We measured the samples at two orthogonal polarizations of the incident light thus characterizing the dependence of their reflectance from the polarization of the incident

light. The BRDF of all samples Black Si, Fractal black and Z306 was measured at wavelengths of 632.8nm and 1064nm, incident angle of 10deg, and viewing angles from -60° to 60° in steps of 5°. The 632.8nm data are plotted in Fig.7, whereas the results at 1064nm are plotted in Fig.8.

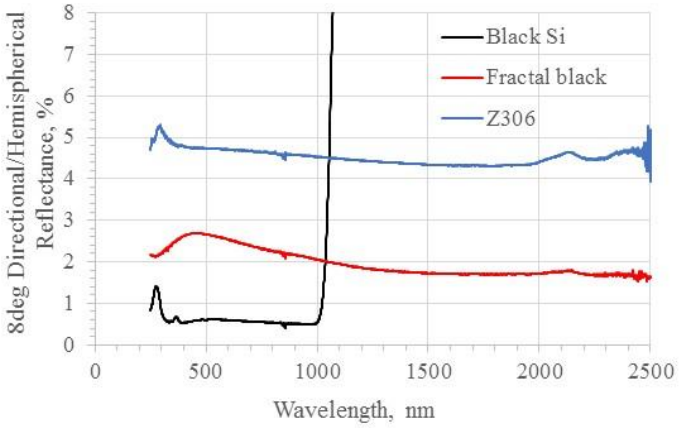

Fig.6 8° Directional/hemispherical reflectance of Black Si, Fractal black and Z306

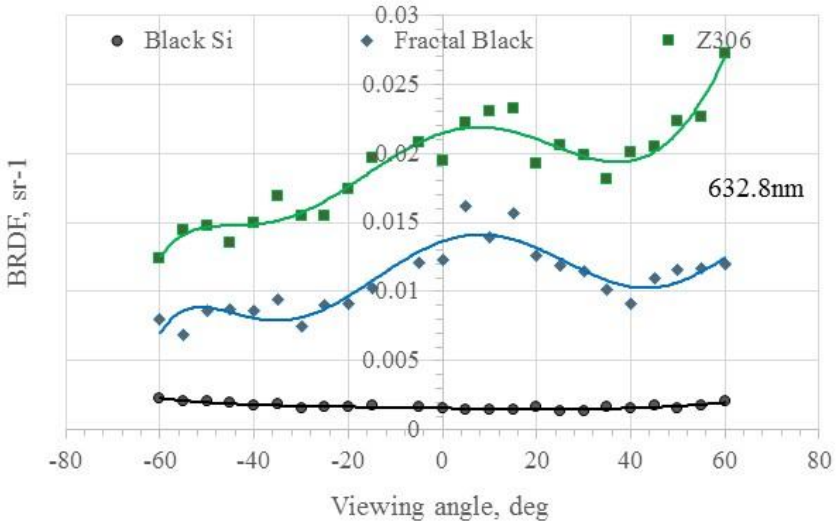

Fig.7 BRDF at 632.8nm, AOI=10°, viewing angles from -60° to 60° of Black Si, Fractal black and Z306, measured points and polynomial fitting

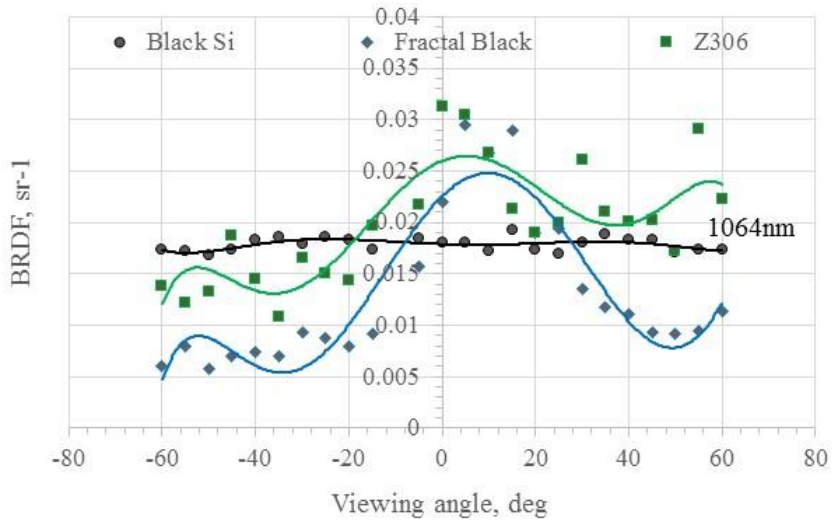

Fig.8 BRDF at 1064nm, AOI=10°, viewing angles from -60° to 60° of Black Si, Fractal black and Z306, measured points and polynomial fitting

Since integration of the 8° directional/hemispherical reflectance over the complete scattering hemisphere of a sample produces that sample's BRDF, the BRDF data shown in figures 7 and 8 follow the directional hemispherical reflectance data. That is, the directional/hemispherical and BRDF data predict the Black Si sample to be the darkest, followed by the Fractal black and Z306 samples. Interesting effects are seen in the BRDF data in the vicinity of the 10° viewing angle, i.e. the direction of specular reflection. Deviation from constant BRDF in these curves is an indication of non-Lambertian reflectance behavior. The Z306 sample shows the largest and sharpest specular reflectance followed by the Fractal black sample at 632.8nm. On the other hand, the Fractal black sample has the highest specular reflectance at 1064nm followed by the Z306. The Black Si sample has the lowest specular reflectance at both wavelengths.

Sources of specular reflection in these samples include reflection off the coating itself and reflection off the base substrate material. Z306 paint exhibits the highest BRDF at both 632.8nm and 1064 nm, while the Black Si exhibits the most Lambertian behavior. The BRDF of the Fractal black and Z306 demonstrate forward scattering properties at 632.8nm and at 1064nm. The Black Si exhibits virtually no forward scatter and retroscatter, characteristic of a near Lambertian scattering surface. Both the Fractal black and Z306 samples exhibit decreasing reflectance at angles away from specular, then the reflectance increases due to forward scattering properties of these materials at both 632.8nm and 1064nm. However, the Black Si sample does not show appreciable reflectance peaks. The specular reflectance most often originate from the top surface of the sample, as in the case with Z306. This is characteristic of a one-bounce surface scattering process. In contrast, the Black Si performs as a very good volume diffuser with multiple reflections within the coating. Interestingly, there is no evidence of retroscatter in the Black Si sample. Retroscatter, if present, would originate from reflectance off the illuminated interior sides of the coating's structure. The lack of retroscatter indicates that light illuminating inside of the coating structure is undergoing multiple internal reflections.

Additional testing was done in order to quantify the specularity of the Black Si. The sample directional reflectance was measured at a 10° incident angle at632.8nm and 1064nm with much

higher sampling frequency as shown in Fig.9 and Fig.10, respectively. No specular peak is evident for the case of the Black Si sample.

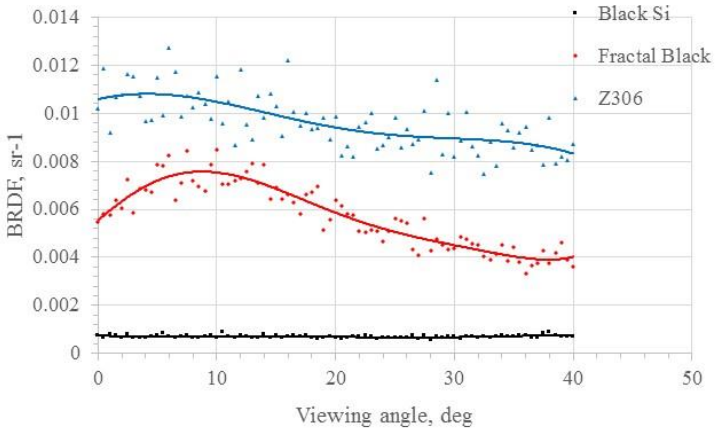

Fig.9 BRDF at 632.8nm, AOI=10°, viewing angles from 0° to 40° step 0.5° of Black Si, Fractal black and Z306, measured points and polynomial fitting

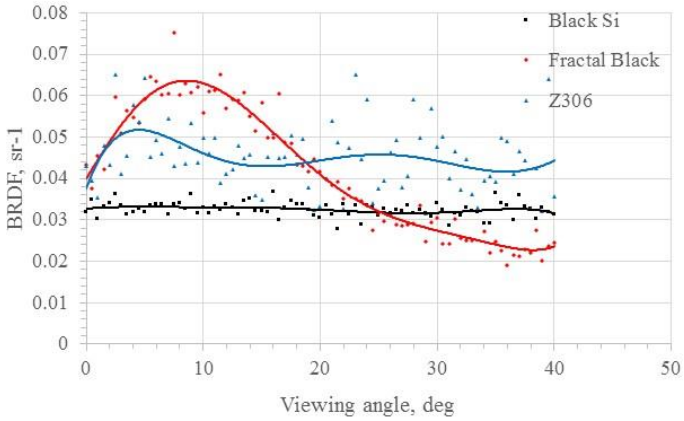

Fig.10 BRDF at 1064nm, AOI=10°, viewing angles from 0° to 40° step 0.5° of Black Si, Fractal black and Z306, measured points and polynomial fitting

The goal of this research was to utilize Black Si in an effort to achieve an order of magnitude lower reflectance as exhibited by Lambertian black coatings and surface treatments currently employed in spacecraft instrument stray light control. From the 8° directional/hemispherical reflectance data, a significant reduction of approximately one order of magnitude reflectance over Z306 paint was realized from 250nm to 1000nm. For the Fractal black sample over the same spectral range, the reduction in reflectance was from 3 to 5 times. In order to realize an order of magnitude reduction in reflectance in the ultraviolet through near infrared, several approaches for optimization of Black Si geometry are being examined. In parallel with current work in reducing the overall reflectance from Black Si samples, research on the reduction of sample specular reflectance is underway in addition to the acquisition of more extensive BRDF measurements at additional wavelengths, incident, and scatter angles.

4. CONCLUSIONS

Initial studies of Black Si structures deposited on the substrates presented in this paper show potential for lowering stray and scattered light in optical instrumentation. Black Si, created by etching on silicon substrate was found to be an order of magnitude darker in the spectral range from 250nm to 1000nm than Z306, a commonly used black paint used in spacecraft instrument applications. It is also much darker than Fractal black used in the aerospace instrumentation. The Black Si sample exhibit practically none specular reflection at 632.8nm and 1064nm. There is no evidence of retroscatter in the Black Si sample. The Black Si reflectance distribution is very close to Lambertian at the two wavelengths we measured. The work presented in this paper constitutes only the initial steps in examining the potential of using Black Si in spacecraft instrument stray light suppression applications. Significant engineering and testing is required to ultimately optimize and qualify Black Si formulations for space use. Elements of this environmental validation effort are currently underway.

5. References

[1] Spergel, D., et al., "Wide-Field InfraRed Survey Telescope-Astrophysics Focused Telescope Assets WFIRST-AFTA," 2015, Science Definition Team (SDT) Wide-Field Infrared Survey Telescope (WFIRST) mission Study Office Report, pp. 1-319.

[2] Pompea, S.M. and R.P. Breault, "Characterization and Use of Black Surfaces for Optical Systems," Chapter 6 in the *Handbook of Optics, Vol. IV*, Optical Properties of Materials, M. Bass, ed., McGraw Hill, pp. 6.1-6.67, 2010

[3] McCall, S.H.C.P., S.M. Pompea, R.P.Breault, and N.L. Regens, "Reviews of Black Surfaces for Space and Ground-based Optical Systems," *Proc. SPIE, 1753, 158-170, 1992*

[4] Persky, M.J., "Review of Black Surfaces for Space-borne Infrared Systems," Rev. Sci. Instrum. 70, 2193-2217, 1999.

[5] Butler J.J., Georgiev G.T., Tweekrem, J.L., Quijada M., Getty S., Hagopian J.G., "Initial studies of the bidirectional reflectance distribution function of carbon nanotube structures for stray light control applications", *Proc. SPIE, Earth Observing Missions and Sensors: Development, Implementation, and Characterization*, vol.7862, 78620D, Oct. 13-14, 2010, Incheon, Korea.

[6] Hagopian J.G., Getty S., Quijada M., Tweekrem, J.L., Shiri R., Roman P., Butler J.J., Georgiev G.T., Livas J., Hunt C., "Multiwalled carbon nanotubes for stray light suppression in space flight instruments", Proc. SPIE, Carbon Nanotubes, Graphene and Associated Devices III, vol.7761, 77610F, Aug.1-5, 2010, San Diego, CA, USA.

[7] K. Balasubramanian, et al., "WFIRST-AFTA coronagraph shaped pupil masks: design, fabrication, and characterization", Journal of Astronomical Telescopes, Instruments, and Systems 2(1), 011005 (Jan–Mar 2016).

[8] Ron S. Shiri, Christine Jhabvala, Georgi Georgiev, Alyssa Barlis, Rémi Soummer, Peter Petrone III, Marc Kuchner, Edward Wollack, Michael Biskach, Timo Saha, Will Zhang, and James Butler, "Highly absorptive pupil mask fabricated with black silicon", Advanced Telescopes and Instruments, SPIE 1116-51, August 2019.

[9] F.E. Nicodemus. J.C. Richmond, J.J. Hsia, I. N. Ginsberg, and T. Limperis, "Geometrical Considerations and Nomenclature for Reflectance," NBS Monograph 160, October 1977.